Computers and Electronics in Agriculture 180 (2021) 105906

Contents lists available at ScienceDirect

Computers and Electronics in Agriculture

journal homepage: www.elsevier.com/locate/compag

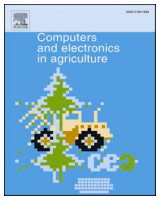

Original papers

DropLeaf: A precision farming smartphone tool for real-time quantification of pesticide application coverage

Bruno Brandoli [a,*], Gabriel Spadon [c,*], Travis Esau [b,*], Patrick Hennessy [b,*], Andre C.P. L. Carvalho [c], Sihem Amer-Yahia [d], Jose F. Rodrigues-Jr [d,c,*]

[a] Department of Computer Science, Dalhousie University, Halifax, NS, Canada
[b] Department of Engineering, Faculty of Agriculture, Dalhousie University, Truro, NS, Canada
[c] Institute of Mathematics and Computer Science, University of Sao Paulo, Sao Carlos, SP, Brazil
[d] CNRS, University of Grenoble, Grenoble-Alpes, France

ARTICLE INFO

Keywords:
Deposition analysis
Spray coverage characterization
Water sensitive papers and cards
UAVs spray
Smart sprayers
Precision farming

ABSTRACT

Pesticides have been heavily used in the cultivation of major crops, contributing to the increase of crop production over the past decades. However, in many cases their appropriate use and calibration of machines rely upon dated evaluation methodologies that cannot precisely estimate how well the pesticides' are being applied to the crop. A few strategies have been proposed in former works, yet their elevated costs and low portability do not permit their wide spread adoption. This work introduces and experimentally assesses a novel tool that functions as a smartphone-based mobile application, named DropLeaf - Spraying Meter. Tests performed using DropLeaf demonstrated that, notwithstanding its simplicity, it can estimate the pesticide coverage with high precision. Our methodology is based on the development of custom image analysis software for real-time assessment of spraying deposition of water-sensitive papers. The proposed tool can be extensively used by farmers and agronomists carrying regular smartphones, improving the utilization of pesticides with well-being, ecological, and monetary advantages. DropLeaf can be easily used for spray drift assessment of different methods, including emerging unmanned aerial vehicle and smart sprayers.

1. Introduction

The total world population is estimated to be 7 billion individuals, with a projection of expanding to 9.2 billion by 2050. This expansion will require almost 70% more nourishment because of changes in diet – more dairy and grains – in underdeveloped countries (Food and Organization, 2009). To adapt to such circumstances, it is obligatory to expand the efficiency of the existing cultivation areas, which might be accomplished by a more reliable food chain, and by the utilization of pesticides (Cooper and Dobson, 2007; Kesterson et al., 2015; Wang et al., 2019). Pesticides are chemical compounds used for killing weed plants (herbicides), parasitic (fungicides), or insects (insecticides) (Bon et al., 2014). The utilization of pesticides is spread around the world, representing a $40 billion yearly budget (Popp et al., 2013) with high concentration of synthetic compounds (approximately 2 kg per hectare (Liu et al., 2015)) being sprayed over a wide range of harvests to augment the production of food. Current evidence suggests that farming will confront heavier stress from pests, prompting a higher interest for pesticides (Popp et al., 2013).

To minimize the risk of crop losses because of herbivorous insects and mites, most of the world's commercial food production systems are subject to several applications of pesticides before being cropped (Cooper and Dobson, 2007; Berenstein and Edan, 2018). Increased usage of real-time automatic section control on agricultural sprayers has led to significant pesticide reductions for farmers (Batte and Ehsani, 2006; Luck et al., 2010; Sharda et al., 2011; Esau et al., 2016). Smart sprayers use sensors to detect and spray pesticide spot-specifically in real-time using individual nozzle control (Esau et al., 2018; Partel et al., 2019). In this situation, it is significant that the right measure of pesticide be sprayed on the harvest fields. Excessive amounts of chemicals may leave residues in the produced food alongside ecological tainting (Gonzalez-Rodriguez et al., 2008; Farha et al., 2018; Witton et al., 2018). If insufficient doses are used there may be areas of the harvest field that are not protected, lessening productivity (Dougoud et al., 2019). For

* Corresponding authors.
E-mail addresses: brunobrandoli@dal.ca, brunobrandoli@gmail.com (B. Brandoli), gabriel@spadon.com.br (G. Spadon), tesau@dal.ca (T. Esau), patrick.hennessy@dal.ca (P. Hennessy), junio@icmc.usp.br (J.F. Rodrigues-Jr).

https://doi.org/10.1016/j.compag.2020.105906
Received 29 August 2020; Received in revised form 13 November 2020; Accepted 16 November 2020
Available online 8 December 2020

instance, Raj et al. (2012) investigated that spray droplet size is key in the efficacy of pesticides against *Asian citrus psyllid*. Meanwhile, irregular spray coverage might cause pest and/or weed resistance, or behavioral avoidance (Renton et al., 2014; Martini et al., 2012). Many fertilizers are often applied as liquid solutions sprayed onto plant leaves and soil (Marcal and Cunha, 2008); to assess their pulverization, it is important to quantify the spray coverage, that is, the relative zone secured by the pesticide droplets – usually composed of water carrier, active ingredients, and adjutant. In today's precision agriculture, several papers investigate the spray drift from agricultural pesticide sprayers and their consequential economic and environmental effects (Preftakes et al., 2019).

The issue of estimating the spray coverage refers to calculating how much pesticide was showered on each piece of the harvest field. The standard way to do that is to disseminate oil- or water-sensitive papers along with the soil and underplant leaves. Then, such cards are covered with a bromoethyl dye that turns blue within the presence of liquid (Giles and Downey, 2003). The issue progresses towards surveying each card by tallying the number of droplets per unit area, by drawing their size distribution, and by evaluating the level of the card area that was covered; these measures enable one to gauge the volume of showered pesticide per unitary area of the harvest. If done manually, this procedure is inefficient and may miss some areas. This is when automatic solutions become essential, including the Swath Kit (Mierzejewski, 1991), a pioneer computer-based procedure that utilizes image processing to asses the water-sensitive cards; the USDA-ARS system (W.C. and A.J., 2005), a camera-based framework that uses 1-cm^2 samples from the cards to form a pool of sensor information; the DropletScan (R. E., 2003), a flatbed scanner defined over a proprietary equipment; the DepositScan framework, made of a workstation and a handheld card scanner (Zhu et al., 2011); and the AgroScan System[1], a Windows-based software that analyzes the collected cards. Every one of these frameworks are inconvenient to convey all through the field, requiring the collection, scanning, and post-processing of the cards, a tedious and labor-intensive procedure.

An option for image capturing systems is to address the characterization of spray application by using wired or remote sensors (Crowe et al., 2005; Giles and Crowe, 2007). However, those are costly and necessitate constant maintenance. Very recently, Wang et al. (2019) implemented a novel droplet deposit sensing system based on a sensor to store the deposition. Then, the Q-Learning algorithm Watkins and Dayan (1992) is used to accurately determine the droplet parameters from UAVs (Unmanned Aerial Vehicles). In 2019, Wang et al. (2019) implemented a new capacitor sensor system for measuring the spray deposit of herbicide application. Moreover, several non-imaging spray methods have been developed for spray analysis by means of non-intrusive characterization, such as phase doppler particle analyzers (PDPA) (Nuyttens et al., 2009), piezoelectric sensors (Gargari et al., 2019), laser diffraction analyzers (e.g., Malvern analyzers (Stainier et al., 2006)), and optical array probes (Teske et al., 2002). All of them designed to assess the quality of spray coverage, including the droplets' size and volume.

Alternatively, a number of image-based approaches have been introduced to assess the efficiency of the spraying deposition quality. Such means profit from the advanced innovations found in smartphones (Xia et al., 2015), which convey computing assets powerful enough to enable a wide scope of uses. In the form of a smartphone application, an image-based system is conceivable as a promptly-accessible tool, portable up to the harvest field, to help growers and agronomists in estimating the spray coverage and, consequently, in decisions concerning where and how to pulverize. This is the point of the present investigation, wherein we present DropLeaf - Spraying Meter [2], a wireless application ready to gauge the measure of pesticide showered on water-sensitive papers. DropLeaf enables precision agriculture, with the potential to improve the evaluation of pesticide showering. It utilizes the phone's camera to register pictures of the spray cards and, nearly immediately, it creates evaluations of the spray coverage using methods based on image processing.

In this context, SnapCard was the first pesticide spray coverage tool developed for running over a smartphone (Nansen et al., 2015; Ferguson et al., 2016). Nevertheless, it presents two drawbacks: i) it calculates the coverage area of the water-sensitive paper only, and ii) it does not allow the user to load a photo from the phone's gallery. Dropcard with DropScope is a similar and commercial smartphone application that relies on an external water-card reader; currently, it works under restricted card sizes. Table 1 compares our proposed solution to the other smartphone applications developed for measuring spraying coverage. It is worth pointing that the smartphone application named Gotas (Chaim et al., 1999) is not covered since it was discontinued.

2. Methodology

In this section, we introduce our methodology, named DropLeaf, to estimate the pesticide spray coverage. The goal is to quantify the coverage area of water-sensitive papers or spray cards, so to help to estimate how adequate the pesticide pulverization was, as discussed in Section 1. DropLeaf builds upon image processing strategies developed on a portable application that is practical on commodity mobile phones. The tool draws three standard measures (W.C. and A.J., 2005) from the drops observed on the spray cards, producing a numerical summary that allows assessing of the spraying:

- **Coverage Area (CA)**: given in percentage of the covered area;
- **Volumetric Median Diameter (VMD)**: given by the 50th percentile $D_{V0.5}$ of the diameter distribution;

Table 1
Comparison of different smartphone applications developed for pesticide spraying assessment using water-sensitive paper.

Smartphone Application	Cost and Platform	Advantages	Limitations
DropLeaf Machado et al. (2018) Website	free, Android	- elaborated user interface - it calculates several statistical measures - it works with any card size - it exports the card measurements	- it runs over Android only - the user must load the card previously cropped using an external photo editor
SnapCard Nansen et al. (2015) Website	free, Android and iOS	- elaborated user interface - it runs over both Android and iOS platforms - it saves the card measurements	- it calculates the coverage area over the water-sensitive paper only - it does not allow the users to load card photos from the gallery
DropCard with DropScope Website	commercial, Android	- it calculates several statistical measures - it saves additional information based on reports	- it demands additional hardware to read the cards - the segmentation of bigger drops fails - it does not load from the photo gallery, hampering the reproduction of previous analyses - it just reads cards of size 7.6 cm × 2.6 cm - it runs over Android only

[1] http://www.agrotec.etc.br/produtos/agroscan/.
[2] The website can be accessed at http://dropleaf.icmc.usp.br/.

- **Relative Span (RS)**: given by $RS = \frac{D_{V0.9} - D_{V0.1}}{D_{V0.5}}$, where $D_{V0.1}$ is the 10th percentile and $D_{V0.9}$ is the 90th percentile of the diameter distribution.

These three measures drive the estimation of the amount of the field covered with pesticide and how well the pesticide was scattered; finer diameters and higher coverage areas indicate a better scattering.

To figure out those measures, it is important to gauge the diameter (in micrometers) of each drop observed on a given card. Manually, this is an arduous task that might take hours per card. To mitigate that, DropLeaf utilizes an intricate image processing method that saves time and provides higher accuracy when contrasted to manual examination and previous systems.

Fig. 1 shows the image processing of DropLeaf, which comprises of six steps carried over a given spray card: (I) color space conversion; (II) binary noise removal; (III) morphological operation of skeletonization; (IV) thresholding; (V) identification of droplets via the marker-based watershed algorithm; and (VI) visualization. We clarify each step indicating why it was necessary and how it identifies with the subsequent step. To illustrate the processing steps, we use a running sample whose picture is exhibited in Fig. 1(a).

2.1. Grayscale transformation

After the acquisition of an image via the cellphone camera $I_{original}(x, y) = (R_{xy}, G_{xy}, B_{xy}) \in [0,1]^3$, Step 1 converts it to a grayscale image $I_{gray}(x, y) \in [0,1]$. This is necessary to ease the discrimination of the card surface from the drops that fell on it. We use the continuous domain of [0,1] so that our formalism can express any color depth; specifically, we use 32 bits for RGB and 8 bits for grayscale. Color information is not needed as it would make the computation heavier and more complex. This first step then transforms the image into a grayscale representation, see Fig. 1 (b), according to:

$$I_{gray}(x, y) = 0.299 * R_{xy} + 0.587 * G_{xy} + 0.114 * B_{xy} \quad (1)$$

2.2. Binarization

Here, the grayscale image I_{gray} passes through a threshold-based binarization process – Step 2, a usual step for image segmentation. Since the grayscale is composed of a single color channel, we achieve binarization by choosing a threshold value. Gray values $I_{gray}(x, y)$ below the threshold becomes black, while above the threshold becomes white. Since spray cards are designed to stress the contrast between the card and the drops, the threshold value is set as a constant value – we use value 0.35 corresponding to value 90 in the 8-bit domain [0,255]. This is a choice that removes noise, and that favors faster processing if compared to more elaborated binarization processes like those based on clustering or on gray-levels distribution. Fig. 1(c) depicts the result, an image $I_{binary}(x, y) \in \{0, 1\}$ given by:

$$I_{binary}(x, y) = \begin{cases} 0, & \text{if } I_{gray}(x, y) < 0.35 \\ 1, & \text{otherwise} \end{cases} \quad (2)$$

2.3. Skeletonization

At this point, we need to identify marks that will spot each drop individually – Step 3. We use the morphology operation of distance transform considering the Euclidean norm and a scale factor of 3 (Gonzalez and Woods, 2007). This algorithm will set the intensity of the white pixels proportional to the distance to their closest black pixel, that is, to the closest drop boundary. The result is a skeleton that emphasizes the inner regions of the drops. Formally, we produce an image $I_{skeleton}$ according to:

$$I_{skeleton}(x, y) = min(\sqrt{(x - x')^2 + (y - y')^2}), \quad \forall\ (x', y') \in I_{binary},\ (x', y') = 0 \quad (3)$$

We normalize the distances computed during the skeletonization using min–max, after which all the pixels' intensities lie within the range [0,1] – see Fig. 1(d).

2.4. Thresholding

Next, we refine the skeleton image to mark the positions of the drops properly. We use a filter based on a threshold value t, which the user can interactively redefine it according to the number and structure of drops. After that, only the strongest most central pixels of each drop will remain in the image, as illustrated in Fig. 1(e)

$$I_{markers}(x, y) = \begin{cases} 0, & \text{if } I_{skeleton}(x, y) < t \\ (x, y), & \text{otherwise} \end{cases} \quad (4)$$

2.5. Marker-based watershed segmentation

In the last step – Step 4, with the drops properly marked on the image, we proceed to the drop identification considering the previously identified contours. To this end, we used the marker-based watershed segmentation. Watershed (Vincent and Soille, 1991) is a technique that considers an image as a topographic relief in which the gray level of the pixels corresponds to their altitude. The transform proceeds by

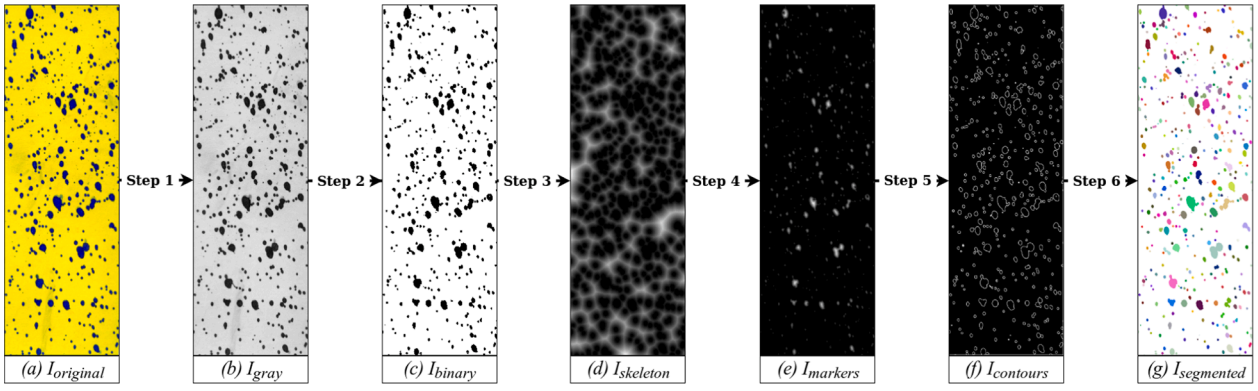

Fig. 1. The image processing course of DropLeaf. It begins by loading an image of a water-sensitive paper. Then, we perform a color-space transformation to obtain a grayscale version of the image – **Step 1**. Subsequently, the grayscale image is binarized to isolate the drops and to remove noise – **Step 2**. Next, we apply the morphological operation of skeletonization – **Step 3**, after which we apply a thresholding operation so to emphasize the drops' markers – **Step 4**. Finally, we use the markers to find the contours of the drops using the marker-based watershed algorithm – **Step 5**, providing the tool with a well-defined set of droplets – visualized after **Step 6**.

simulating the flooding of a landscape starting at the local minima. This process forms basins that are gradually fulfilled with water. Eventually, the water from different basins meet, indicating the presence of ridges (boundaries); this is an indication that a segment was found and delimited. The process ends when the water reaches the highest level in the color-encoding space. The problem with the classical watershed is that it might over-segment the image in the case of an excessive number of minima. For better precision, we use the marker-controlled variation of the algorithm proposed by Gaetano et al. (2012). This variation is meant for images in which the shapes are previously marked. Given the markers, the marker-based watershed proceeds by considering as minima only the pixels within the boundaries of the markers. Watershed is an iterative algorithm computationally represented by a function *watershed(Image i, Image[] markers)*. We use such a function to produce a set of segments (drops) over the gray-level image I_{gray} while considering the set of markers identified in the image $I_{markers}$, as follows:

$$contours[] = watershed(I_{gray}, findContours(I_{markers})) \quad (5)$$

where $Image[]findContours(Imagei)$ is a function that, given an image, returns a set of sub-images corresponding to the markers; watershed is a function that, given an input image and a set of markers corresponding to subsets of pixels, produces a set of segments stored in an array of contours, which we illustrate in Fig. 1(f).

We use the product of watershed to produce our final output $I_{segmented}$ by drawing the segments over the original image, as illustrated in Fig. 1 (g). Notice that the last image, $I_{segmented}$, is meant only for visualization. The statistical analysis over the drops' shapes is computed over the set of segments.

2.6. Diameter processing

After the segmentation, we have a set of segments, each corresponding to a drop of pesticide. The final step is to compute the measures presented at the beginning of this section: coverage area (CA), volumetric median diameter (VMD), and relative span (RS). Since we have the segments computationally represented by an array of binary matrices, we can calculate the area and the diameters of each drop by counting the pixels of each matrix. After counting, it is necessary to convert the diameter given in pixels into a diameter given in micrometers (μm), which, for the i-th drop, goes as follows:

$$diameter_{\mu m}(drop_i) = width_{px}(drop_i) * \frac{width^{card}_{\mu m}}{width^{card}_{px}} \quad (6)$$

where, $width_{px}(drop_i)$ is the width in pixels of the *i*-th drop; $width^{card}_{px}$ is the width of the card in pixels; and $width^{card}_{\mu m}$ is the width of the card in micrometers. Notice that we used *width*, but we could have used *height* as well; what matters is that the fraction provides a conversion ratio given in $px/\mu m$, which is not sensitive to the axis; horizontal or vertical, the ratio is the same for a non-distorted image.

Notice that we obtain $width_{px}(drop_i)$ and $width^{card}_{px}$ via image processing, after the segmentation method; meanwhile, $width^{card}_{\mu m}$ is a constant provided by the user, corresponding to the real-world width of the card. Also, notice that we are considering that the diameter corresponds to the horizontal axis (the width) of the drop; it is possible, however, that the diameter corresponds to the vertical axis, in which case the formulation is straightly similar. Choosing between the horizontal and the vertical axes might be tricky in case the drop is elliptical, rather than circular. We solved this issue by extracting the diameter from the area of the drop. We use the formula of the circle area $a_{circle} = \pi * radius^2 = \pi * (\frac{diameter}{2})^2$. With simple algebra, we conclude that given the area in pixels of the *i*-th drop, its diameter in pixels is given by the following equation:

$$diameter_{px}(drop_i) = 2 * \sqrt{\frac{area_{px}(drop_i)}{\pi}} \quad (7)$$

Rewriting Eq. (6) by means of Eq. (7), we get:

$$diameter_{\mu m}(drop_i) = 2 * \sqrt{\frac{area_{px}(drop_i)}{\pi}} * \frac{width^{card}_{\mu m}}{width^{card}_{px}} \quad (8)$$

The metrics standard to droplet analysis, as listed in Section 2, are given in diameter unit. Hence, at this point, it is necessary to convert the area of the droplets as identified by DropLeaf into their circular diameter-descriptive counterpart. To do so, we apply Eq. (8), which derives from algebraically rewriting Eqs. (6) and (7) together.

2.7. Implementation

The use of mobile devices to perform automatic tasks has increased fast (Xia et al., 2015). The reasons are the recent advances in hardware, such as sensors, processors, memories, and cameras. Thereby, smartphones have become platforms for applications of image processing and computer vision (Giovanni Maria et al., 2015; Machado et al., 2016).

Mobile devices are adequate to perform real-time tasks *in situ*, far from the laboratory. In this context, besides the methodology, the contribution of this work is the development of a mobile application to measure the quality of pesticide spraying on water-sensitive cards. For implementation, we partly used methods from the OpenCV library[3], and Java was the programming language. The application is fully functional, as depicted in Fig. 2, and available in the Google Play platform at https://play.google.com/store/apps/details?id=upvision.dropleaf.

3. Experimental results

In this section, we evaluate our methodology in measuring the spray coverage deposition. The goal is to correctly measure the spray drops both in terms of density (drops/cm^2) and of drop diameter.The first set of experiments was conducted over reference cards. The second set of experiments was conducted over real water-sensitive cards, demonstrating that the application works even during *in situ* conditions.

3.1. Control-card experiments

We use the reference card provided by the *Agrotechnical Advisory* of German enterprise *Hoechst*. The card has synthetic drops with sizes 50 μm, 100 μm, 250 μm, 500 μm, and 1,000 μm, as shown in Fig. 3. It is used to calibrate equipment and to assess the accuracy of manual and automatic measuring techniques. Since the number and sizes of drops are known, this first experiment works as a controlled validation.

To measure the drops, we used a smartphone to capture the image of the card. In Table 2, we present the average diameter of the drops, the area covered by the drops given in μm^2, the density given in drops per cm^2, the coverage area given in percentage of the card area, and the volumetric median diameter. We do not present the volumetric median and the relative span because, as all the drops are equal, these values become not significant. From the table, we conclude that the accuracy of the methodology is in accordance with the controlled protocol; that is, the known and measured diameters match in most of the cases. Notice that it is not possible to achieve a perfect identification because of printing imperfections and numerical issues that inevitably rise at the micrometer scale. For example, for 1,000 μm drops, the average diameter was 1,009 μm. This first validation was necessary to test the ability of the tool in telling apart card background and drops.

Still using the control card, Table 3 compares the coverage area and

[3] http://opencv.org.

Fig. 2. Screenshots of our fully-functional app. Freely available for download on GooglePlay.

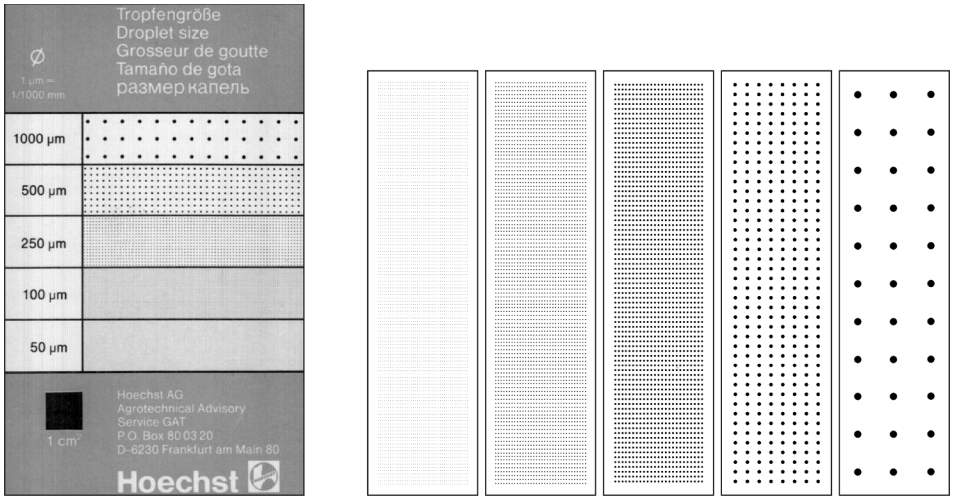

Fig. 3. Control card provided by *Hoechst*. Each card has synthetic drops with sizes varying from 50 µm, 100 µm, 250 µm, 500 µm, to 1,000 µm, respectively.

Table 2
DropLeaf drop identification over the control card by enterprise *Hoechst*.

Dropleaf				
Diameter (µm)		Area (μm^2)	Density (drops/cm^2)	Coverage Area (%)
Controlled	Measured			
50	58	2,693	594.31	5.32%
100	141	15,687	399.01	15.01%
250	246	53,470	229.73	23.46%
500	467	214,970	37.20	11.8%
1,000	1,009	901,811	3.65	3.72%

the average diameter measured by DropLeaf, by tool DepositScan, and by a stereoscopic microscope (provided in the work of Zhu et al. (2011)).

The results demonstrated that the DropLeaf performed slightly better compared with a stereoscopic microscope for different diameters, excepted for 500 µm (see erros in Table 3), followed by results of DepositScan. DropLeaf presented the best results after the microscope, beating the precision of DepositScan for all the drop sizes, but 500 µm; for 1,000 µm drops, the two tools had a similar performance, diverging in less than 1%. In the experiments, one can notice that the bigger the drop, the smaller the error, which ranged from 41% to less than 1%. For bigger drops, the drop identification is next to perfect using DropLeaf. When measuring drops as small as 50 µm, a single extra pixel detected by the camera is enough to produce a big error. This problem was also observed in the work of Zhu et al. (2011).

By analyzing the data, we concluded that the error due to the size scale is predictable. Since it varies with the drop size, it is not linear; nevertheless, it is a pattern that can be corrected with the following general equation:

$$diameter' = a*diameter^{b} \quad (9)$$

Table 3
DropLeaf compared to tool DepositScan and a stereoscopic microscope with respect to the control card.

Diameter (μm)	DropLeaf			DepositScan			Microscope		
	Area (μm²)	Diameter (μm)	Error	Area (μm²)	Diameter (μm)	Error	Area (μm²)	Diameter (μm)	Error
50	2,693	58	16%	6,093	88	76%	3,390	66	32%
100	15,687	141	41%	21,505	165	65%	15,906	142	42%
250	53,470	246	1.6%	52,688	259	3.6%	45,342	240	4%
500	214,970	467	6.6%	196,236	500	0%	201,924	507	1.4%
1,000	901,811	1,009	0.9%	777,954	995	0.5%	797,752	1,008	0.8%

In the case of our tool, we used $a = 0.2192733$ and $b = 1.227941$. These values shall vary from method to method, as we observed for DepositScan and the stereoscopic microscope.

3.2. Card experiments

In the second set of experiments, we used six cards evaluated in the work of Cunha et al. (2012). Similar to them, we categorized the cards into three groups of two cards, which we classified as sparse, medium, and dense with respect to the density of drops, as seen in Fig. 4. These experiments tested our methodology by assessing its ability in identifying drops even when they are irregular and/or they have touching borders. Table 4 shows the numerical results, including the number of drops, the coverage area, the density, the coverage area, the volumetric median diameter, and the relative span.

It is necessary to interpret the table along with Fig. 4, which presents the drops as identified by our methodology. In the figure, it is possible to inspect the four first measures visually. It is also possible to see that the right-hand side images (the tool's results stressed with colored drops) demonstrate that the segmentation matches the expectations of a visual inspection; the drops at the left are perfectly identified on the right. The colormap used in the visual segmentation of droplets is essentially performed by assigning a predefined range of colors to the vector containing the drops ordered according to size. For the first version of Dropleaf, we enumerated each drop taking into account the position into the ordered vector, but the enumeration got completely scattered in terms of spatial position and, additionally, the number was so tiny in some drops that we could not see the labels on the mobile's screen.

Other features are also noticeable; density, for instance, raises as we visually inspect Fig. 4(a) through Fig. 4(f); the corresponding numbers in the table raise similarly. Counting the number of drops requires close attention and much time; for the less dense Figs. 4(a) and 4(b), however, one can verify the accuracy of the counting and segmentation. It is worth noticing that droplets vary their shape regarding the impact, speed and direction from drop projecting through the air onto the card and, are usually seen as scattered spatter that can once had colided in the air. Nonetless, the user can vary the threshold value according to the density of drops in the card. We tested values from 10 to 25, with step of 1. Values higher than 25 tends to create a misleaded segmentation, and values between 17 and 23 tend to produce best results. We tested our tool with value set at 17, however, users can change that and vissually assess that.

The last two measures, VMD and RS, provide parameters to understand the distribution of the drops' diameters. For example, one can see that, being denser, cards (e) and (f) had a smaller median and a larger span of diameters. These measures indicate that the spraying is irregular and that it needs adjustment. Meanwhile, cards (a) and (b) are more regular, but not as dense as desired, with a lot of blank spots. Cards (c) and (d), in turn, have more uniform spraying and more regular coverage.

4. Fractal analysis

In this section, we present early experiments related to using fractal theory in the task of expressing the spraying pattern of droplets on a water-sensitive paper.

4.1. Fractal theory

Fractal geometry provides a mathematical model for complex objects found in nature. In contrast to the Euclidean geometry, the fractal dimension assumes that an object might have a non-integer dimensionality. Estimating the fractal dimension of an object is essentially related to its complexity, which can be measured in terms of how it occupies the space. For instance, the fractal dimension has been applied in texture analysis and shape measurement (Machado et al., 2013). Although there are different methods for calculating the fractal dimension, the box-counting method is the most frequently used for measurements in various application fields – specifically, the spray-card problem is particularly adherent to the box-counting method. Its procedure is as follows:

$$D = 2 - \lim_{\sigma \to 0} \frac{log\, N(\sigma)}{log\,(1/\sigma)} \tag{10}$$

where $N(\sigma)$ is the least number of boxes of length σ to completely cover

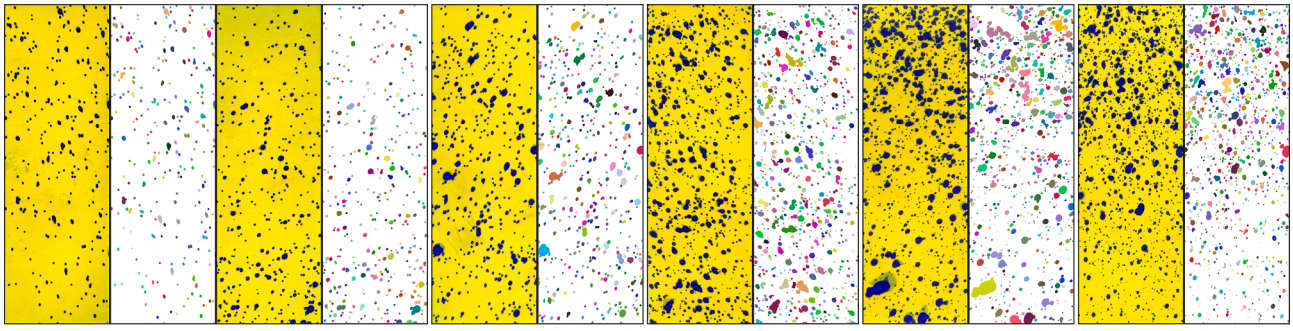

Fig. 4. Drop identification over cards used in a real crop. We categorized the cards as: sparse – images (a) and (b); medium – images (c) and (d); and dense – images (e) and (f). The ones on the left are the original cards, and at the right are the segmented cards. The output is a colormap assigned to the vector containing the drop size segmented in order to visually differentiate them.

Table 4
Drop assessment over cards used in a real crop.

	Dropleaf					
Sample	Drops	Area (μm²)	Density (drops/cm²)	Coverage Density (%)	Volumetric Median Diameter (μm)	Relative Span
sparse (a)	255	250,138	12.90	4.54	452	1.22
sparse (b)	359	261,464	18.16	6.45	425	1.55
medium (c)	448	355,712	22.67	9.99	448	1.83
medium (d)	444	357,005	22.46	9.71	428	2.22
dense (e)	923	364,749	46.71	18.22	246	3.75
dense (f)	1,150	215,090	58.19	15.44	239	3.40

the object, scaled down by a ratio of $1/\sigma$. Given a binary image of $M \times M$ pixels, where M is a power of 2, first generate a set of box sizes σ for laying grids on the image. Subsequently, each grid becomes a box of size $\sigma \times \sigma$ and the number of boxes $N(\sigma)$ needed to completely cover the object is counted. Finally, the limit is calculated using the linear regression of the curve $\log 1/\sigma \times \log N(\sigma)$. The fractal dimension is computed by $D = 2 - |\alpha|$, where α is the slope of the estimated line.

4.2. Spraying pattern analysis

In this experiment, we analyzed images of water-sensitive paper by means of fractal dimension. Our goal was to find evidence that the space occupation of droplets on a water-sensitive paper has a relationship to its fractal dimensionality. In Fig. 5, we present experiments carried over nine different real samples. In the figure, one can see that the fractal dimension is highly correlated to quantitative spraying measures of coverage area (%) and volume (uL/m^3). The conclusion is straight: the higher the value of the fractal dimension, the higher the coverage area and the volume of sprayed pesticide. This early conclusion allows us to speculate about using the fractal dimension as one single quantitative measure to describe the regularity of droplets overs water-sensitive paper.

5. Discussion of results

This section examines issues as when creating advances for spray card investigation. We confronted such issues during our work; here, we examine them as a further contribution to aid scientists dealing with the same or related aspects.

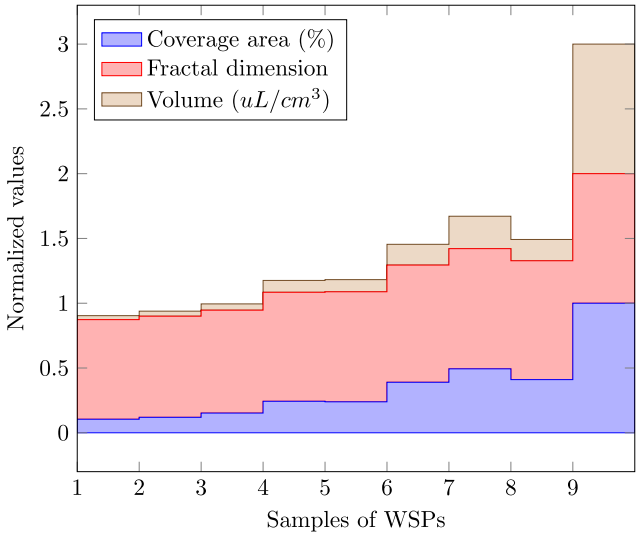

Fig. 5. The plot of nine samples of water-sensitive paper. One can observe the correlation among measures of coverage area, volume, and fractal dimension. The x-axis corresponds to the number of the sample; the y-axis corresponds to the normalized output of values of the three measures.

5.1. Coverage factor

After our experiments, we observed that when the spraying gets excessively thick, it is not possible to properly detect the drops, regardless of which system is utilized for estimation; data about the number of drops, and their diameter distribution, for example, cannot be cast any longer. This impact was brought up by Fox et al. (2003), who claims that an absolute coverage of the card above 20% leads to questionable results; and a coverage with 70% of coverage is unfeasible regarding analysis. This is due to the fact that, with an excessive amount of spraying, the drops fall excessively close, causing overlaps; visually, it is like two or more drops become one. This phenomenon occurs because of the intermolecular attractions present in the water drops, which makes them combine, shaping greater drops.

As a result, caution is required, regardless of which procedure of assessment, whenever the absolute coverage region sums up over 20%, a situation when the measurements lose accuracy, and one can depend only on the coverage area for basic decision making. Despite the fact that the diameter is not measurable, the enormous drops that may be observed demonstrate an intemperate measure of pesticide and/or a malfunctioning of the spray device. It's recommended that a combination of both assessing the number of droplets as well as the total coverage area is done to ensure accurate decisions. This is especially important when using anti-drift nozzles or lower nozzle pressures which typically provide larger diameter droplet sizing.

5.2. Angle of image capture

We likewise observed that, for all the research done so far, including ours, the image processing technique used to identify the drops works only if the capture angle of the card photo is of 90 degrees. That is, the viewing angle of the camera/scanner must be orthogonal to the spray card surface. This is important in light of the fact that the pixels of the picture are converted into real-world dimensions to express the diameter of the drops in μm; that is, it is vital that the components of the picture be homogeneous concerning scale. In the event that the capture angle is not proper, the picture becomes misshaped, producing different scales in each region of the picture. For flatbed scanners, this is direct to ensure; notwithstanding, for handheld gadgets (cameras and cell phones), extra care is required. In such cases, one may require a special protocol to capture the image, such as utilizing a tripod. This issue may likewise be solved by methods of image processing, which demand extra research and experimentation. PDF scanning apps such Microsoft Office Lens[4], Adobe Scan[5], and CamScanner[6] can automatically crop and rescale off-angle pictures of paper to appear as if the images were captured at 90

[4] https://play.google.com/store/apps/details?id=com.microsoft.office.officelens.
[5] https://play.google.com/store/apps/details?id=com.adobe.scan.android.
[6] https://play.google.com/store/apps/details?id=com.intsig.camscanner.

degrees. This concept could be adapted for scanning water-sensitive spray cards within DropLeaf; however, the results of rescaled pictures may have additional error compared to pictures captured orthogonally.

5.3. Minimum dots per inch (dpi)

Our trials additionally showed that there must be a minimum amount of data on the spray card pictures so as to accomplish the ideal accuracy with respect to the drops' diameters. This minimum is expressed by the *dots per inch* (dpi) property of the imaging process; dpi is a well-known resolution measure that communicates how many pixels are required to represent one inch in the real-world, as for example, when hardcopy printing. If insufficient pixels are caught per inch of the spray card, it winds up difficult to estimate the width of the tiniest drops. This may impact the diameter distribution analysis concealing issues in the spraying procedure.

To refine our conclusions, we experimented on the minimum dpi that is fundamental for each drop diameter. In Table 5, one can see the minimum number of pixels to express each drop diameter for each dpi value; see that a few cells of the table are vacant (loaded up with a hyphen) showing that the diameter cannot be computationally represented in that dpi resolution. Likewise, see that, in the columns, the number of pixels for one same diameter increments with the resolution. Clearly, the more data, the more accuracy at the expense of more processing power, considerable more storage, and more system transmission demands when transferring pictures. From the table, it is conceivable to reason that 600 dpi is the minimum resolution for robust analyses, since it can represent diameters as small as 50 μm; meanwhile, a resolution of 1,200 dpi, albeit more robust, might prompt downsides with respect to the administration of image files that are too huge. In any case, even if a resolution is sufficient to represent a given diameter, it is not assured that drops with that diameter will be detected; this comes from the fact that the image detection relies upon different factors, for example, the nature of the focal points, and the image processing algorithm.

Table 5 is a guide for developers willing to computationally analyze spray cards, and furthermore for agronomists who are choosing which hardware to purchase in the face of their needs. Nonetheless, We evaluated the image processing over Android smartphones – LG-H873, Motorola XT1540, Motorola XT1952–4, Samsung SM-J320W8 – and each needed approximately 1 s to perform the entire processing procedure on a single sample image. An Android tablet (Acer A1-810) needed approximately 3 s. This shows the feasibility of running the Dropleaf on smartphones.

Table 5
Pixels needed to represent a given length, given a dpi. The length of 10 um, for example, demands 1 pixel to be represented in a 2600 dpi resolution, and cannot be represented in a smaller resolution; the length of 10,000 um demands 20 pixels in a mere 50 dpi resolution.

μm | *dpi*	50	100	300	600	1200	2400	2600
10	-	-	-	-	-	-	1
50	-	-	-	1	2	5	5
100	-	-	1	2	5	9	10
250	-	1	3	6	12	24	26
500	1	2	6	12	24	47	51
1,000	2	4	12	24	47	94	102
10,000	20	39	118	236	472	945	1024

6. Conclusions

This paper presents DropLeaf, a portable application to quantify pesticide spray coverage via image processing of water-sensitive spray cards. It was demonstrated that the accuracy of DropLeaf was sufficient to permit the utilization of mobile phones as substitutes for costly, cumbersome, and time-consuming equipment. The approach was instantiated in a freely-accessible tool to be utilized in the assessment of real-world crops, which provides in-field results for expediated sprayer management decisions – https://play.google.com/store/apps/details?id=upvision.dropleaf. We experimented with the tool with two datasets of water-sensitive papers; our investigations exhibited that DropLeaf tracks drops with high precision, producing standard metrics for quantifying the pesticide coverage. Moreover, our portable application identifies overlapping drops, a significant improvement with respect to former methods. This is because by providing a finer precision, the tool produces not only better accuracy, but also more information. DropLeaf can be used in a range of applications related to farming, including the evaluation of emerging innovations of agricultural machines based on unmanned aerial vehicles and smart sprayers. The information provided by DropLeaf is useful for calibrating system pressure, flow rate, and travel speeds for sprayers. Properly calibrating these parameters increases desired ecological effects of the spray application, limits unwanted spray drift, and optimizes the use of pesticide inputs to limit costs. Dropleaf is an innovative tool beneficial for not only traditional sprayers but also the ever-increasing use of unmanned aerial or ground vehicles.

Declaration of Competing Interest

The authors declare that they have no known competing financial interests or personal relationships that could have appeared to influence the work reported in this paper.

Acknowledgements

The authors are thankful to Dr. Claudia Carvalho who kindly provided annotated cards; to Brazilian agencies Fundacao de Apoio a Pesquisa do Estado de Sao Paulo (grants 2019/04461-9, 2018/17620-5, 2017/08376-0, and CEPID CeMEAI grant 2013/07375-0); to the Conselho Nacional de Desenvolvimento Cientifico e Tecnologico (grant 167967/2017-7, 406550/2018-2, 305580/2017-5, and 05580/2017-5); and to the Coordenacao de Aperfeicoamento de Pessoal de Nivel Superior - Finance Code 001.

References

Batte, M.T., Ehsani, M.R., 2006. The economics of precision guidance with auto-boom control for farmer-owned agricultural sprayers. Comput. Electron. Agric. 53, 28–44. https://doi.org/10.1016/j.compag.2006.03.004. URL http://www.sciencedirect.com/science/article/pii/S0168169906000366.

Berenstein, R., Edan, Y., 2018. Automatic adjustable spraying device for site-specific agricultural application. IEEE Trans. Autom. Sci. Eng. 15, 641–650. https://doi.org/10.1109/TASE.2017.2656143.

Bon, H., Huat, J., Parrot, L., Sinzogan, A., Martin, T., Malezieux, E., Vayssieres, J.F., 2014. Pesticide risks from fruit and vegetable pest management by small farmers in sub-saharan africa. a review. Agron. Sustainable Develop. 34, 723–736.

Chaim, Ademir, Maia, Aline Holanda Nunes, Pessoa, Maria Conceição Peres Young, 1999. Estimates of pesticide deposition by droplet size analysis. Pesquisa Agropecuária Brasileira 34, 962–969. https://doi.org/10.1590/S0100-204X1999000600006. URL http://www.scielo.br/scielo.php?script=sci_arttext&pid=S0100-204X1999000600006&nrm=iso.

Cooper, J., Dobson, H., 2007. The benefits of pesticides to mankind and the environment. Crop Protect. 26, 1337–1348. https://doi.org/10.1016/j.cropro.2007.03.022. URL http://www.sciencedirect.com/science/article/pii/S026121940700097X.

Crowe, T.G., Downey, D., Giles, D.K., 2005. Digital device and techinique for sensing distribution of spray deposition. Transactions of the ASABE -. Am. Soc. Agric. Biol. Eng. 48, 2085–2093. https://doi.org/10.13031/2013.20085. URL http://elibrary.asabe.org/abstract.asp?aid=20085&t=3.

Cunha, M., Carvalho, C., Marcal, A.R., 2012. Assessing the ability of image processing software to analyse spray quality on water-sensitive papers used as artificial targets. Biosyst. Eng. 111, 11–23. https://doi.org/10.1016/j.biosystemseng.2011.10.002. URL http://www.sciencedirect.com/science/article/pii/S1537511011001772.

Dougoud, J., Toepfer, S., Bateman, M., Jenner, W.H., 2019. Efficacy of homemade botanical insecticides based on traditional knowledge. a review. Agron. Sustainable Develop. 39, 37. https://doi.org/10.1007/s13593-019-0583-1.

Esau, T., Zaman, Q., Groulx, D., Corscadden, K., Chang, Y., Schumann, A., Havard, P., 2016. Economic analysis for smart sprayer application in wild blueberry fields. Precision Agric. 17, 753–765. https://doi.org/10.1007/s11119-016-9447-8.

Esau, T., Zaman, Q., Groulx, D., Farooque, A., Schumann, A., Chang, Y., 2018. Machine vision smart sprayer for spot-application of agrochemical in wild blueberry fields. Precision Agric. 19, 770–788. https://doi.org/10.1007/s11119-017-9557-y.

Farha, W., Abd El-Aty, A.M., Rahman, M.M., Jeong, J.H., Shin, H.C., Wang, J., Shin, S.S., Shim, J.H., 2018. Analytical approach, dissipation pattern and risk assessment of pesticide residue in green leafy vegetables: A comprehensive review. Biomed. Chromatogr. 32, 4134–4141. https://doi.org/10.1002/bmc.4134. URL http://arxiv.org/abs/https://onlinelibrary.wiley.com/doi/pdf/10.1002/bmc.4134, arXiv: https://onlinelibrary.wiley.com/doi/pdf/10.1002/bmc.4134</hi></xref>.

Ferguson, J.C., Chechetto, R.G., O'Donnell, C.C., Fritz, B.K., Hoffmann, W.C., Coleman, C.E., Chauhan, B.S., Adkins, S.W., Kruger, G.R., Hewitt, A.J., 2016. Assessing a novel smartphone application - snapcard, compared to five imaging systems to quantify droplet deposition on artificial collectors. Comput. Electron. Agric. 128, 193–198. https://doi.org/10.1016/j.compag.2016.08.022. URL http://www.sciencedirect.com/science/article/pii/S016816991630182X.

Food, Organization, A., 2009. Feeding the world in 2050. Technical Report. United Nations. World agricultural summit on food security.

Fox, R., Derksen, R., Cooper, J., Krause, C., Ozkan, H., 2003. Visual and image system measurement of spray deposits using water sensitive paper. Appl. Eng. Agric. 19, 549–552.

Gaetano, R., Masi, G., Scarpa, G., Poggi, G., 2012. A marker-controlled watershed segmentation: Edge, mark and fill, in. In: 2012 IEEE International Geoscience and Remote Sensing Symposium (IGARSS). IEEE, pp. 4315–4318.

Gargari, H.P., Teimourlou, R.F., Valizadeh, M., 2019. Spray droplet characterization using a piezoelectric sensor through classification based on machine learning. Agric. Eng. 59, 151–160. https://doi.org/10.35633/INMATEH-59-17.

Giles, D., Crowe, T., 2007. Real-time electronic spray deposition sensor. http://www.google.com.br/patents/US7280047. uS Patent 7,280,047.

Giles, D.K., Downey, D., 2003. Quality control verification and mapping for chemical application. Precision Agric. 4, 103–124.

Giovanni Maria, F., Daniele, R., Valeria, T., Mirko, G., Sebastiano, B., 2015. Representing scenes for real–time context classification on mobile devices. Pattern Recogn. 48, 1086–1100. https://doi.org/10.1016/j.patcog.2014.05.014.

Gonzalez, R.C., Woods, R.E., 2007. Image processing. Digital image processing 2.

Gonzalez-Rodriguez, R.M., Rial-Otero, R., Cancho-Grande, B., Simal-Gandara, J., 2008. Determination of 23 pesticide residues in leafy vegetables using gas chromatography and ion trap mass spectrometry and analyte protectants. J. Chromatogr. A 1196–1197, 100–109. http://www.sciencedirect.com/science/article/pii/S0021967308004056, doi: 10.1016/j.chroma.2008.02.087.

Kesterson, M.A., Luck, J.D., Sama, M.P., 2015. Development and preliminary evaluation of a spray deposition sensing system for improving pesticide application. Sensors 15, 31965–31972. https://doi.org/10.3390/s151229898. URL http://www.mdpi.com/1424-8220/15/12/29898.

Liu, Y., Pan, X., Li, J., 2015. A 1961–2010 record of fertilizer use, pesticide application and cereal yields: a review. Agron. Sustainable Develop. 35, 83–93.

Luck, J., Pitla, S., Shearer, S., Mueller, T., Dillon, C., Fulton, J., Higgins, S., 2010. Potential for pesticide and nutrient savings via map-based automatic boom section control of spray nozzles. Comput. Electron. Agric. 70, 19–26. https://doi.org/10.1016/j.compag.2009.08.003. URL http://www.sciencedirect.com/science/article/pii/S0168169909001586.

Machado, B.B., Casanova, D., Gonçalves, W.N., Bruno, O.M., 2013. Partial differential equations and fractal analysis to plant leaf identification. J. Phys: Conf. Ser. 410, 012066. https://doi.org/10.1088/1742-6596/410/1/012066.

Machado, B.B., Orue, J.P.M., Arruda, M.S., Santos, C.V., Sarath, D.S., Goncalves, W.N., Silva, G.G., Pistori, H., Roel, A.R., Rodrigues-Jr, J.F., 2016. Bioleaf: A professional mobile application to measure foliar damage caused by insect herbivory. Comput. Electron. Agric. 129, 44–55. https://doi.org/10.1016/j.compag.2016.09.007. URL http://www.sciencedirect.com/science/article/pii/S0168169916307670.

Machado, B.B., Spadon, G., Arruda, M.S., Goncalves, W.N., Carvalho, A.C.P.L.F., Rodrigues-Jr, J.F., 2018. A smartphone application to measure the quality of pest control spraying machines via image analysis. In: Proceedings of the 33rd Annual ACM Symposium on Applied Computing, ACM, New York, NY, USA. pp. 956–963. URL http://doi.acm.org/10.1145/3167132.3167237, doi:10.1145/3167132.3167237.

Marcal, A.R.S., Cunha, M., 2008. Image processing of artificial targets for automatic evaluation of spray quality. Trans. ASABE 51, 811–821. URL http://asae.frymulti.com/toc.asp.

Martini, X., Kincy, N., Nansen, C., 2012. Quantitative impact assessment of spray coverage and pest behavior on contact pesticide performance. Pest Manag. Sci. 68, 1471–1477.

Mierzejewski, K., 1991. Aerial spray technology: possibilities and limitations for control of pear thrips. Technical Report. U.S. Department of Agriculture, Forest Service. Tech. Rep. NE-147.

Nansen, C., Ferguson, J.C., Moore, J., Groves, L., Emery, R., Garel, N., Hewitt, A., 2015. Optimizing pesticide spray coverage using a novel web and smartphone tool, snapcard. Agron. Sustainable Develop. 35, 1075–1085. https://doi.org/10.1007/s13593-015-0309-y.

Nuyttens, D., De Schampheleire, M., Verboven, P., Brusselman, E., Dekeyser, D., 2009. Droplet size and velocity characteristics of agricultural sprays. Trans. ASABE 52, 1471–1480.

Partel, V., Kakarla, S.C., Ampatzidis, Y., 2019. Development and evaluation of a low-cost and smart technology for precision weed management utilizing artificial intelligence. Comput. Electron. Agric. 157, 339–350. https://doi.org/10.1016/j.compag.2018.12.048. URL http://www.sciencedirect.com/science/article/pii/S0168169918316612.

Popp, J., Peto, K., Nagy, J., 2013. Pesticide productivity and food security. a review. Agron. Sustainable Develop. 33, 243–255.

Preftakes, C.J., Schleier, Jerome J, r., Kruger, G.R., Weaver, D.K., Peterson, R.K.D., 2019. Effect of insecticide formulation and adjuvant combination on agricultural spray drift. PeerJ 7, 7136–7156. https://doi.org/10.7717/peerj.7136. URL https://pubmed.ncbi.nlm.nih.gov/31249737.

Raj, B.D., Masoud, S., Siddharth, T., Kirsten, P.S., L., S.L., 2012. Spray droplet size affects efficacy of fenpropathrin against asian citrus psyllid. In: Bernards, M. (Ed.), Pesticide Formulations and Delivery Systems: Innovating Legacy Products for New Uses, ASTM International, Tampa, Florida, USA. pp. 1–13. doi:10.1520/STP104310.

R.E., W., 2003. Assessing the ability of dropletscan to analyze spray droplets from a ground operated sprayer. Appl. Eng. Agric. 19, 525–530.

Renton, M., Busi, R., Neve, P., Thornby, D., Vila-Aiub, M., 2014. Herbicide resistance modelling: past, present and future. Pest Manag. Sci. 70, 1394–1404.

Sharda, A., Fulton, J.P., McDonald, T.P., Brodbeck, C.J., 2011. Real-time nozzle flow uniformity when using automatic section control on agricultural sprayers. Comput. Electron. Agric. 79, 169–179. https://doi.org/10.1016/j.compag.2011.09.006. URL http://www.sciencedirect.com/science/article/pii/S0168169911002092.

Stainier, C., Destain, M.F., Schiffers, B., Lebeau, F., 2006. Droplet size spectra and drift effect of two phenmedipham formulations and four adjuvants mixtures. Crop Protect. 25, 1238–1243. https://doi.org/10.1016/j.cropro.2006.03.006. URL http://www.sciencedirect.com/science/article/pii/S0261219406000627.

Teske, M.E., Thistle, H.W., Hewitt, A.J., Kirk, I.W., 2002. Converison of droplet size distributions from pms optical array probe to malvern laser difraction. Atomizat. Sprays 12, 267–281.

Vincent, L., Soille, P., 1991. Watersheds in digital spaces: an efficient algorithm based on immersion simulations. IEEE Trans. Pattern Anal. Machine Intell. 13, 583–598.

Wang, L., Yue, X., Liu, Y., Wang, J., Wang, H., 2019. An intelligent vision based sensing approach for spraying droplets deposition detection. Sensors 19. https://doi.org/10.3390/s19040933. URL https://www.mdpi.com/1424-8220/19/4/933.

Wang, P., Yu, W., Ou, M., Gong, C., Jia, W., 2019. Monitoring of the pesticide droplet deposition with a novel capacitance sensor. Sensors 19. https://doi.org/10.3390/s19030537. URL https://www.mdpi.com/1424-8220/19/3/537.

Watkins, C.J., Dayan, P., 1992. Q-learning. Machine Learn. 8, 279–292.

W.C., H., A.J., H., 2005. Comparison of three imaging systems for water-sensitive papers. Appl. Eng. Agric. 21, 961–964.

Witton, J.T., Pickering, M.D., Alvarez, T., Reed, M., Weyman, G., Hodson, M.E., Ashauer, R., 2018. Quantifying pesticide deposits and spray patterns at micro-scales on apple (malus domesticus) leaves with a view to arthropod exposure. Pest Manag. Sci. 74, 2884–2893. https://doi.org/10.1002/ps.5136. URL https://onlinelibrary.wiley.com/doi/abs/10.1002/ps.5136, arXiv:https://onlinelibrary.wiley.com/doi/pdf/10.1002/ps.5136.

Xia, F., Hsu, C.H., Liu, X., Liu, H., Ding, F., Zhang, W., 2015. The power of smartphones. Multimedia Syst. 21, 87–101. https://doi.org/10.1007/s00530-013-0337-x.

Zhu, H., Salyani, M., Fox, R.D., 2011. A portable scanning system for evaluation of spray deposit distribution. Comput. Electron. Agric. 76, 38–43.